

Lawrence Berkeley National Laboratory

Lawrence Berkeley National Laboratory

Title

Elimination of 'ghost'-effect-related systematic error in metrology of X-ray optics with a long trace profiler

Permalink

<https://escholarship.org/uc/item/4wv3w2tx>

Authors

Yashchuk, Valeriy V.
Irick, Steve C.
MacDowell, Alastair A.

Publication Date

2005-04-28

Elimination of ‘ghost’-effect-related systematic errors in metrology of X-ray optics with a long trace profiler

Valeriy V. Yashchuk*, Steve C. Irick, Alastair A. MacDowell
Lawrence Berkeley National Laboratory, 1 Cyclotron Road, Berkeley, CA, USA 94720

ABSTRACT

A data acquisition technique and relevant program for suppression of one of the systematic effects, namely the ‘ghost’ effect, of a second generation long trace profiler (LTP) is described. The ‘ghost’ effect arises when there is an unavoidable cross-contamination of the LTP sample and reference signals into one another, leading to a systematic perturbation in the recorded interference patterns and, therefore, a systematic variation of the measured slope trace. Perturbations of about 1-2 μrad have been observed with a cylindrically shaped X-ray mirror. Even stronger ‘ghost’ effects show up in an LTP measurement with a mirror having a toroidal surface figure. The developed technique employs separate measurement of the ‘ghost’-effect-related interference patterns in the sample and the reference arms and then subtraction of the ‘ghost’ patterns from the sample and the reference interference patterns. The procedure preserves the advantage of simultaneously measuring the sample and reference signals. The effectiveness of the technique is illustrated with LTP metrology of a variety of X-ray mirrors.

Keywords: trace profiler, systematic error reduction, X-ray optics, metrology

1. INTRODUCTION

The long trace profiler (LTP) is a basic metrology tool for highly accurate testing of the figure of X-ray optics with slope variations on the order of one micro-radian rms¹⁻⁴. The LTP records the local slope profile of a surface by measuring the reflection angle of a laser sample beam as the beam is transported across the surface by an air bearing carriage. Due to the translation of the optical sensor, the LTP has a unique capability for surface figure metrology of very long, meter size, mirrors⁵⁻⁷. However, non-idealities of the translation mechanism as well as non-idealities of the optical elements bring forth a number of systematic effects, which often dominate over the random noise of the LTP measurement⁸⁻¹⁰. Some of the systematic effects have been analyzed and the methods for their suppression have been developed¹¹⁻¹⁴. Beginning with the second generation LTP systems, a reference arm in addition to the sample arm is used^{15,16}. The optical schematic of the reference arm is identical to the sample arm and both arms use essentially the same optical elements with the exception of a small flat reference mirror for the reference arm. Measuring the angle of reflection from the reference mirror allows monitoring the systematic errors related to laser pointing instability and carriage wiggling.

Here, we describe an improved LTP data acquisition technique, and special software developed to reduce one of the systematic effects named the ‘ghost’ effect. The origin of the ‘ghost’ effect is the unavoidable cross-contamination of the sample and reference signals into one another. The ‘ghost’ effect is significantly increased for a toroidal or a twisted mirror, because the sample light beam moves not only tangentially along the corresponding detector, but also in the sagittal direction, spilling onto the detector for the reference arm lying parallel to it. Without special treatment, the ‘ghost’ effect can cause systematic variations of the measured slope trace of about 1-2 μrad and even more. The effectiveness of the proposed method is illustrated with LTP metrology of a variety of X-ray mirrors.

2. LTP SYSTEMATIC ERROR DUE TO THE ‘GHOST’ EFFECT

The LTP available in the Optical Metrology Laboratory (OML) at the Advanced Light Source (ALS) belongs to the second generation of the LTP systems; it is called an LTP II. The main difference between the LTP II and an instrument of the first generation is the existence of a reference arm in addition to the measurement arm. Figure 1 shows the simplified optical schematic of the LTP II. The system of beam splitter (BS) and two prisms (P1 and P2) splits a laser beam into a pair of collinear beams with a separation of approximately 1 mm. A polarizing beam splitter (PBS) splits

the beam pair into two pairs, one of which is directed to a reference mirror (reference beam) and the other to the sample mirror (sample beam). These two pairs of beams reflected from the sample and the reference mirrors, respectively, pass through a Fourier transform lens (FTL). This lens serves as an angle-to-position converter, by focusing the tilted beams on two position-sensitive linear detectors, PD1 and PD2, that lie adjacent to each other in the sagittal plane. One linear detector is used for the sample beam and the other for the reference beam. In our case, the detectors are linear photo-diode arrays (PDA) of 1024 pixels with a pixel size of $\sim 25 \mu\text{m} \times 2.5 \text{mm}$. One half-wave plate is used for attenuation of the laser light intensity; another one allows for balancing the intensities of the sample and the reference beams. The quarter-wave plates rotate the linear polarization by 90 degrees (for a double pass) in order to redirect the reflected beams to the photo-detectors. In each arm, the light beam is split into two parallel beams, which are made to interfere at the focus of Fourier transform lens.

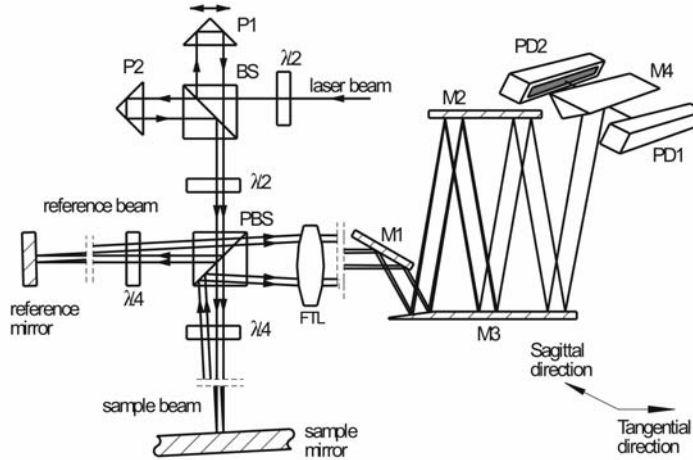


Figure 1: Optical schematic of the LTP. P1 and P2 are adjustable and stationary prisms, respectively; BS is a beam splitter, PBS is a polarizer beam splitter, the half-wave plates are used for attenuation and balancing the beam intensities detected with the position-sensitive photo-detectors – PD1 and PD2; FTL is a Fourier transform lens, which serves as an angle-to-position converter; mirrors M1, M2, and M3 fold the light beams, decreasing the overall size of the LTP optical system; a prism mirror M4 directs the beams to the linear area detectors (PD1 and PD2). For our LTP set-up, the focal length of the Fourier transform lens is $f = 1250 \text{mm}$.

The LTP schematic shown in Fig. 1 is a realization of so called pencil-beam interferometer system developed by K. von Bieren¹⁷. The parallel beams of each pair are made to interfere at the focus of the Fourier transform lens. The sample and the reference beams produce separate spatial patterns of interference fringes on corresponding position-sensitive detectors placed at the focus. An example of the interference fringes measured with a cylindrical mirror with length of 70 mm and radius of curvature of approximately 26.6 m is presented in Fig. 2, where both the sample beam and reference beam are shown overlapped on the same plot. The pattern from each arm has a characteristic two-peak shape. The position of a pattern is defined as the position of the central minimum, and depends on the reflection angle of the beam, i.e. the slope of the reflecting surface is measured. The separation between the sample and reference patterns is a measure of the slope of the mirror surface at the point of measurement. Generally, the reference arm is adjusted to minimize the movement of the reference pattern while measuring. At the same time, if a curved mirror is under investigation, the sample pattern position on the detector changes, sometimes significantly, depending on the surface slope of the mirror. The LTP is calibrated to provide the slope value from the measured beam positions on the detector arrays. In the course of fitting with the LTP software, two slope traces for the sample and reference arms are calculated from the measurements of the interference patterns as the LTP optical head is translated along the tangential direction of a sample mirror. The resulting slope profile plot of the sample mirror surface is generated as a difference of the slope traces for the sample and reference mirrors.

In order to maximally employ the advantage of the reference channel and to avoid the additional systematic effects associated with non perfect sensor optics (the beam splitters, Fourier lens, wave plates, mirrors), it is desired to align the

sample and the reference beams to pass along the same optical path. This however results in low spatial separation between the two beams. The beams have a sagittal height of about 5 mm that together with the detector pixel height of 2.5 mm leads to the cross-contribution of the sample and reference signal into another. We call this cross contamination of the sample and reference signals the ‘ghost’ signal. In practice, the beam alignment is a compromise between the requirements of the same optical path and the separation of the beams on the detectors; and the ‘ghost’ signal is nearly always seen in the measured interference patterns. As the ‘ghost’ signal overlaps with the primary signal, the computed centroid of the pattern changes depending on the relative position of the ‘ghost’ leading to the systematic perturbation in the measured slope trace. For the measurement shown in Fig. 2, the ‘ghost’ overlaps with the reference signal in the $20\text{ mm} < X < 40\text{ mm}$ region of the mirror. This exactly corresponds to the position of the systematic perturbation in the residual slope trace seen depicted with a circle in Fig.3. Figure 3 shows the residual slope trace obtained as a deviation of the difference of the sample and reference traces from the best fit cylinder with curvature radius of 26.64 m. For providing a clear illustration of the “ghost effect” in Figs. 2 and 3, the LTP alignment was not optimized for minimizing the ‘ghost’ effect. When the LTP optics are optimally aligned, the amplitude of the ‘ghost’ features are smaller by approximately a factor of five. Even in this case the slope perturbation can be 1-2 μrad .

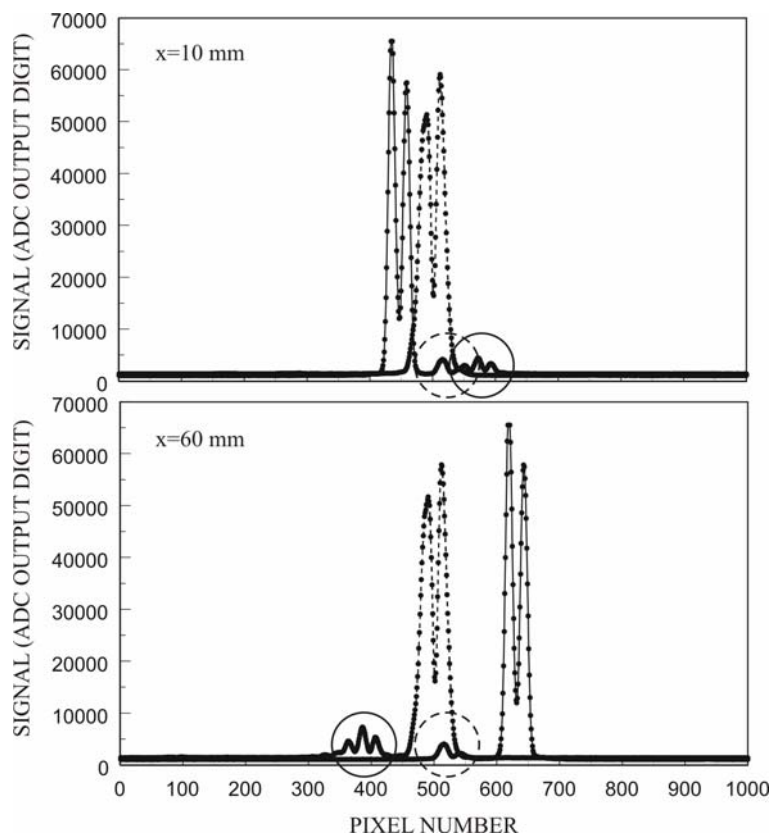


Figure 2: The sample (solid lines) and reference (dashed lines) interference patterns recorded with the LTP. The sample and reference plots are overlaid for these plots. The mirror under investigation has a length = 70mm and a radius of curvature of approximately 26.6 m in the tangential (measuring) direction. The upper plots were measured at a tangential position of $x=10\text{ mm}$ which was the edge of the mirror clear aperture; the lower plots correspond to $x=60\text{ mm}$. During the LTP scan the sample signal moves significantly across the plot, the reference signal in general remains stationary monitoring only laser beam directional changes and stage pitching errors. The circles depict the ‘ghost’ features; the circle line style marks the origin of a ‘ghost’ feature. The pixel separation is $25\text{ }\mu\text{m}$. For providing a clear illustration of the ‘ghost’ effect, the LTP adjustment was not optimized for minimizing the ‘ghost’ effect. When the LTP optics are more optimally aligned, the amplitude of the ‘ghost’ features are smaller approximately by factor of five.

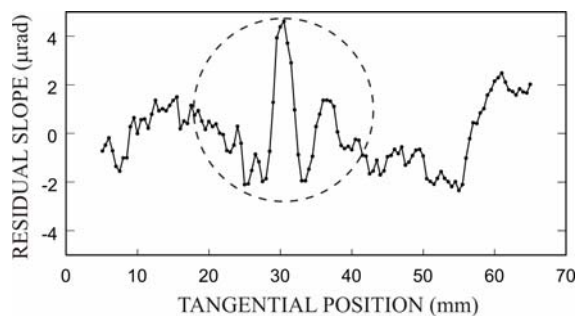


Figure 3: The LTP residual (deviation from the best fit cylinder) slope trace obtained as a difference of the signal traces measured in the sample and in the reference arms. The 70 mm long mirror was cylindrically curved in tangential direction. The extracted effective radius of the mirror curvature is $R=26.64\text{ m}$. The ‘ghost’ perturbation is marked with a circle.

3. LTP DATA ACQUISITION FOR SUPPRESSING THE ‘GHOST’ EFFECT

In order to suppress the ‘ghost’ effect in the present LTP II arrangement, we separately measure the ‘ghost’ features in both arms and then subtract the ‘ghost’ intensities from the corresponding interference patterns. In spite of the triviality of the procedure, its effectiveness for elimination of the ‘ghost’ effect is not obvious. Indeed, the sample and reference patterns, which have to be corrected, are the result of the interference of the light beams, with a certain phase relation. The overlap of the primary light with the ‘ghost’ light should be also thought of as an interference process dependent on the relative phase of the beams and superposition of the corresponding light amplitudes. For the work described here, the proposed method is based on subtraction of the light intensities and the phase relation between the light beams is ignored. The suppression procedure is therefore an approximation and the effectiveness has to be verified experimentally.

The suggested procedure is realized by series of successive LTP measurements. The general sequence of measurements is schematically shown in Fig. 4.

First, the regular intensity file is recorded, containing the data from both the sample, $S_{1,1}(I_x)$, and the reference, $R_{1,1}(I_x)$, arms. Here, the indexes mark the status of the corresponding arm, the first index relates to the sample arm, the second index relates to the reference arm; if index is ‘0,’ the corresponding beam was blocked, if index is ‘1,’ the beam was unblocked. I_x is the interference pattern measured at the position x .

Second, a similar measurement is carried out with the sample beam blocked, $S_{0,1}(I_x)$, $R_{0,1}(I_x)$. In this case, the signal recorded in the sample arm, $S_{0,1}(I_x)$, is due to the light leakage from the reference arm that is the ‘ghost’ in the measurement arm. The signal recorded in the reference arm, $R_{0,1}(I_x)$, has a regular shape.

Third, the measurement is repeated when the reference beam is blocked, $S_{1,0}(I_x)$, $R_{1,0}(I_x)$. Now the signal recorded in the reference arm, $R_{1,0}(I_x)$, is due to the ‘ghost’ light from the measurement beam. The signal recorded in the sample arm, $S_{1,0}(I_x)$, has a regular shape.

Fourth, in order control the possible instrument drift, one more regular LTP measurement is carried out, $S'_{1,1}(I_x)$, $R'_{1,1}(I_x)$.

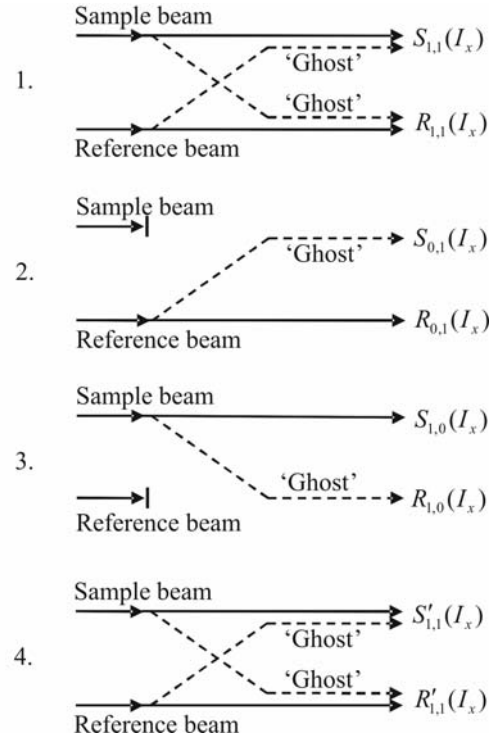


Figure 4: See text.

After the measurements have been performed, the interference patterns measured at the same tangential position are linearly combined in order to subtract the ‘ghost’ effect contributions from the averaged data obtained in the regular LTP arrangement:

$$S_M(I_x) = \frac{1}{2} S_{1,1}(I_x) + \frac{1}{2} S'_{1,1}(I_x) - S_{0,1}(I_x), \text{ and } R_M(I_x) = \frac{1}{2} R_{1,1}(I_x) + \frac{1}{2} R'_{1,1}(I_x) - R_{1,0}(I_x).$$

The modified interference patterns, $S_M(I_x)$ and $R_M(I_x)$, are collected in the modified data file. Then the LTP fitting procedure to find the slope values via the position of minimum of the interference patterns is applied to the modified data¹⁸. A program that allows creating a linear combination of the interference patterns from up to four LTP data files was specially developed. The program named MID.vi (Manual Intensity Data virtual instrument, reference¹⁹) is based on LabView software.

The LTP data acquisition procedure described above differs significantly from the previous “old” procedure in that the measurement of the sample and reference signal traces are made at different times. This places extra demands on the temporal stability and repeatability of the LTP. These have to be more stable than the errors generated by the “Ghost” effect. Below, we demonstrate the effectiveness of the developed procedure.

The effectiveness of the procedure to suppress the systematic error due to the ‘ghost’ effect is illustrated in Fig. 5. The upper plot (Fig. 3a) reproduces the residual slope trace shown in Fig. 3, corresponding to a single regular LTP measurement. The central trace (Fig. 5b) is the result of application of the described procedure to the set of four successive measurements performed in the manner described above. The lower trace (Fig. 5c), which is the difference of the first two traces, is the ‘ghost’-related perturbation of the slope measurement. The ‘ghost’ effect has a significant magnitude for more than a 10 mm long part of the trace that corresponds to approximately the doubled tangential size of the light beam in one of the LTP arms.

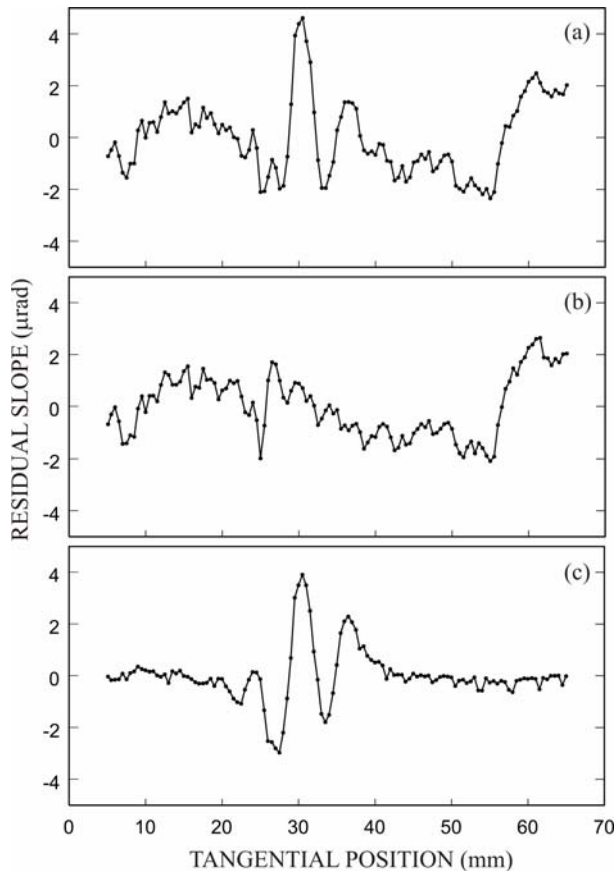


Figure 5: a – the LTP residual (deviation from the best fit cylinder) slopes trace obtained as a difference of the signal traces measured in the sample and in the reference arms. The 70 mm long mirror is cylindrically curved in the tangential direction. The extracted effective radius of the mirror curvature is $R=26.64$ m. b – the residual slope trace resulted from application of the ‘ghost’ effect suppression procedure to the set of four successive measurements performed in the manner described in the text. a – the difference of the traces (a) and (b) that is the ‘ghost’-related perturbation of the slope measurement.

With the developed program, the same set of data was combined into a data file generally free of the ‘ghost’ effect. For this purpose, the measurements with the reference beam blocked and with the sample beam blocked were used as the sample and the reference signal data, respectively. The residual slope trace obtained by fitting the combined data file was subtracted from the trace resulting from the application of the ‘ghost’ effect suppression procedure shown in Fig. 5b. Figure 6 shows the differential trace. A remarkable observation from the differential trace is that there is not any irregular perturbation in the vicinity of the ‘ghost’ effect feature seen in Fig. 5c. This suggests that the contribution of the phase difference interference between the primary beams and the ‘ghost’ beams is negligible at the existing level of accuracy. This also illustrates the efficiency of the ‘ghost’ effect suppression with the developed data acquisition procedure, which can be characterized with a factor of suppression defined as a ratio of amplitudes of the ‘ghost’ effect feature in Fig. 5c and the residual variations seen in the same place in Fig. 6. This gives the suppression factor of about 10. The long spatial variation of the differential slope in Fig. 6 is probably due to slow instrumental drift between the

measurements of the sample and the reference data used to get the combined data file. The differential slope trace in Fig. 6 can also be considered as a proof that the procedure developed preserves the advantage of using the reference arm for monitoring some slow instrumental drifts.

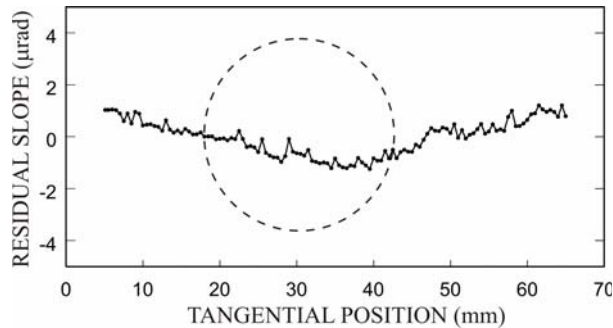


Figure 6: The difference of the slope trace resulted from application of the ‘ghost’ effect suppression procedure (Fig. 5b) and the trace obtained as a combination of two separated measurements while the sample beam was blocked and the reference beam was blocked, respectively. Because there is not an irregular perturbation over the position of the ‘ghost’ feature seen in Fig. 2, the effect of the interference between the primary beams and the ‘ghost’ ones is negligibly small.

4. DISCUSSIONS AND CONCLUSIONS

The developed procedure was successfully used for suppression of the ‘ghost’-effect-related systematic perturbations of the surface slope trace of X-ray mirrors measured with the LTP II. Sometimes, for a mirror with relatively small curvature and length it is possible to adjust the overall tilt of the mirror in such a way that there is no overlap of the primary interference patterns with the ‘ghost’ features at all measured ranges of the slope. However, the adjustment is compromised due to the significant difference of the optical paths for the sample and reference beams, opening a way for the introduction of other systematic errors. Even in this case we found it to be beneficial to use the ‘ghost’ effect suppression procedure instead of over-separating the sample and the reference beams. In the case of a significantly curved mirror, similar to one used for illustration throughout this work, there is an unavoidable ‘ghost’ effect with slope perturbation on the level of 1-2 μrad . The described data acquisition technique provides a powerful tool to reduce these systematic perturbations by an order of magnitude.

The ‘ghost’ effect is significantly increased for a toroidal (curved in the sagittal direction) or a twisted mirror, because the sample light beam is defocused, and the interference feature from the sample arm moves not only tangentially along the corresponding detector array, but also in the sagittal direction, spilling significantly onto the detector of the reference arm. In this case, the magnitude of the ‘ghost’ signal can be comparable with the primary signal.

Figure 7 present an example of such a situation. The interference patterns shown in Fig. 7 were measured with a single crystal silicon X-ray mirror with the length of 370 mm. The mirror is cylindrically shaped in the sagittal direction with a radius of curvature of about 250 mm. The patterns in Fig. 7a and Fig. 7c correspond to the signal in the LTP reference arm recorded in two regular measurements. The feature on the right hand side of the patterns is the ‘ghost.’ It has a size comparable with the primary interference pattern. The measurements correspond to the same tangential position on the mirror surface, $X=170$ mm, where the primary and the ‘ghost’ features were well separated. In the course of the measurement, the features overlapped in such a way that the resulting pattern could not be even fitted with the LTP software. The developed procedure and the relevant software solved the problem. Figure 7b depicts the ‘ghost’ signal measured alone between the regular measurements, while the reference light beam was blocked ($X=170$ mm). The pattern obtained after subtraction of the ‘ghost’ feature from the averaged regular pattern is shown in Fig. 7d. The ‘ghost’ was significantly suppressed providing the possibility to obtain the slope trace via fitting with the LTP software.

In conclusion, the data acquisition procedure described here and the software specially developed allow the reduction of the ‘ghost’-effect-related systematic perturbation of the LTP slope measurement by approximately an order of magnitude. An additional suppression could be achieved with a more sophisticated fitting procedure. In this case, a special shape correction would need to be applied to the ‘ghost’ effect pattern in order to correct the drift-related difference of shape of the ‘ghost’ features measured during and between the regular measurements. The idea of the correction can be illustrated with Fig. 7. The residual ‘ghost’ signal in the lowest plot (Fig 7d) is due to the change of

the shape of the ‘ghost’ features between the measurements. For the data in Fig. 7, the time between two consequent measurements was about 5 min. However, the time of measurement with overlapped primary and ‘ghost’ signals was a few seconds; and the drift for this time was correspondingly smaller. Therefore the shape correction based on comparison of the ‘ghost’ feature shapes before and after overlapping would provide additional suppression of the systematic error.

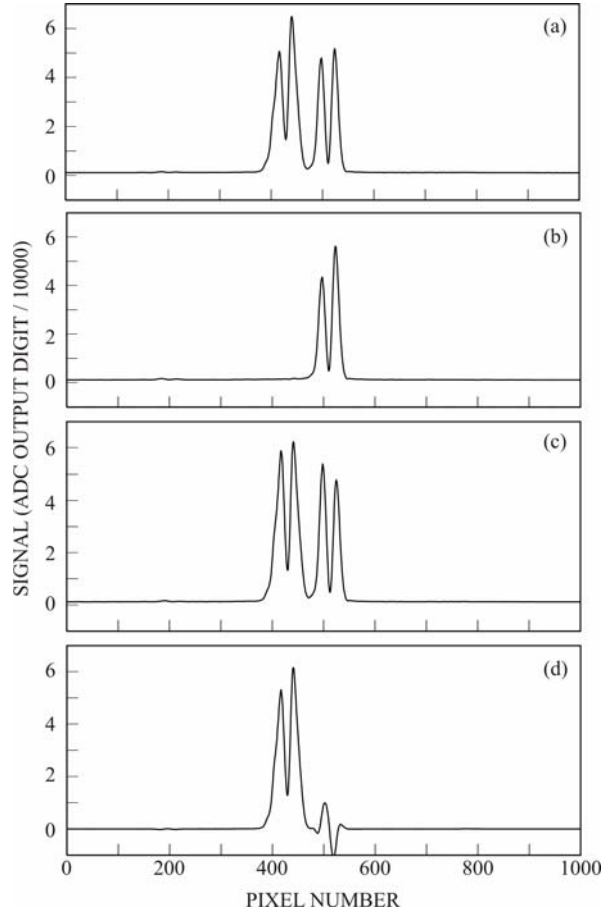


Figure 7: a and c – the interference patterns correspond to the signal in the LTP reference arm recorded in two regular measurements with a mirror cylindrically shaped in sagittal direction. The mirror length was 370 mm and radius of sagittal curvature was approximately 250 mm. b - the ‘ghost’ signal measured alone between the regular measurements, while the reference light beam was blocked; d - the pattern obtained after subtraction of the ‘ghost’ feature from the pattern averaged over the two regular measurements. All the plots correspond to the same tangential position on the mirror surface, $X=170$ mm. The feature on the right-hand side of the patterns relates to the ‘ghost’ effect. It has a size comparable with the primary interference pattern. The pattern obtained after subtraction of the ‘ghost’ feature from the averaged regular pattern is shown in Fig. 7d. The ‘ghost’ is significantly suppressed providing the possibility to obtain the slope trace via fitting with the LTP software. Note that the difference between two regular measurements shown with plots (a) and (c) is due to the slow instrumental drift between the measurements.

ACKNOWLEDGEMENTS

The authors are grateful to W. McKinney, H. Padmore, P. Takacs, and T. Warwick for extremely useful discussions. This work was supported by the U. S. Department of Energy under contract number DE-AC03-76SF00098.

REFERENCES

1. E. L. Church, P. Z. Takacs, *Use of an optical profiling instrument for the measurement of the figure and finish of optical quality surfaces*, *Wear*, 109 (1986), 241-57.
2. P. Z. Takacs, S-N. Qian, J. Colbert, *Design of a long trace surface profiler*, *Proceedings of SPIE 749* (1987), 59-64.
3. P. Z. Takacs, S. K. Feng, E. L. Church, S-N. Qian, W-M. Liu, *Long trace profile measurements on cylindrical aspheres*, *Proceedings of SPIE*, 966 (1989), 354-64.
4. S. C. Irick, W. R. McKinney, *Advancements in one-dimensional profiling with a long trace profiler*, *Proceedings of SPIE*, 1720 (1992), 162-8.
5. S. C. Irick, *Determine surface profile from sequential interference patterns from a long tracer profiler (for synchrotron optics)*, *Rev. Sci. Instrum.* 63(1) (1992) 1432-5.

6. S-N. Qian, H. Li, P. Z. Takacs, *Penta-Prism Long Trace Profiler (PPLTP) for measurement of grazing incidence space optics*, Proceedings of SPIE, 2805 (1996), 108-14.
7. P. Z. Takacs, S-N. Qian, T. Kester, H. Li, *Large-mirror figure measurement by optical profilometry techniques*, Proceedings of SPIE, 3782 (1999), 266-74.
8. S-N. Qian, G. Sostero, P. Z. Takacs, *Precision calibration and systematic error reduction in the Long Trace Profiler*, Proceedings of SPIE, 3782 (1999), 627-36.
9. Shinan Qian, Sostero G, P. Z. Takacs, *Precision calibration and systematic error reduction in the long trace profiler*, Optical Engineering, 39(1) (2000), 304-10.
10. P. Z. Takacs, S-N. Qian, *Accuracy limitations in long-trace profilometry*, AIP Conference Proceedings, 708 (2004), 831-4.
11. S-N. Qian, W. Jark, P. Z. Takacs, *The penta-prism LTP: a long-trace-profiler with stationary optical head and moving penta prism*, Rev. Sci. Instrum. 66(3) (1995), 2562-9.
12. P. Z. Takacs, C. J. Bresloff, *Significant improvements in long trace profiler measurement performance*, Proceedings of SPIE 2856 (1996), 236-45.
13. P. Z. Takacs, E. L. Church, C. J. Bresloff, L. Assoufid, *Improvements in the accuracy and the repeatability of long trace profiler measurements*, Applied Optics, 38(25) (1999), 5468-79.
14. Shinan Qian, P. Z. Takacs, *Equal optical path beamsplitter for a pencil beam interferometer and shearing interferometer*, Optical Engineering 42(no.4) (2003).929-34.
15. S. C. Irick, W. R. McKinney, D. L. Lunt, P. Z. Takacs, *Using a straightness reference in obtaining more accurate surface profiles from a long trace profiler (for synchrotron optics)*, Rev. Sci. Instrum., 63(1) , 1436-8 (1992).
16. S. C. Irick, *Improved measurement accuracy in a long trace profiler: compensation for laser pointing instability*, Nuclear Instruments & Methods in Physics Research A-Accelerators Spectrometers Detectors & Associated Equipment, 347(1-3), 226-30 (1994).
17. K. von Bieren, *Interferometry of wave fronts reflected off conical surfaces*, Applied Optics, 22(4), 2109 (1983).
18. S. C. Irick, *Convention of LTP data file format*, Light Source Note LSBL-718 (ALS, LBNL, Berkeley, October 11, 2000.); <http://www-esg.lbl.gov/Production/OML/LTPpubs.htm>.
19. This program was developed using LabVIEW 7.0; <http://www-esg.lbl.gov/Production/OML>.

*vvyashchuk@lbl.gov; phone +1 510-495-2592; fax +1 510-486-7696